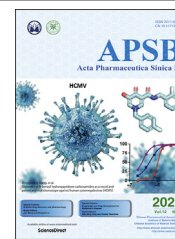




Chinese Pharmaceutical Association
Institute of Materia Medica, Chinese Academy of Medical Sciences

Acta Pharmaceutica Sinica B

www.elsevier.com/locate/apsb
www.sciencedirect.com



ORIGINAL ARTICLE

Validation and invalidation of SARS-CoV-2 main protease inhibitors using the Flip-GFP and Protease-Glo luciferase assays



Chunlong Ma, Haozhou Tan, Juliana Choza, Yuyin Wang, Jun Wang*

Department of Pharmacology and Toxicology, College of Pharmacy, the University of Arizona, Tucson, AZ 85721, USA

Received 26 August 2021; received in revised form 24 September 2021; accepted 14 October 2021

KEY WORDS

SARS-CoV-2;
Antiviral;
Main protease;
Ebselen;
Carmofur;
FlipGFP assay;
Protease-Glo luciferase assay

Abstract SARS-CoV-2 main protease (M^{Pro}) is one of the most extensively exploited drug targets for COVID-19. Structurally disparate compounds have been reported as M^{Pro} inhibitors, raising the question of their target specificity. To elucidate the target specificity and the cellular target engagement of the claimed M^{Pro} inhibitors, we systematically characterize their mechanism of action using the cell-free FRET assay, the thermal shift-binding assay, the cell lysate Protease-Glo luciferase assay, and the cell-based FlipGFP assay. Collectively, our results have shown that majority of the M^{Pro} inhibitors identified from drug repurposing including ebselen, carmofur, disulfiram, and shikonin are promiscuous cysteine inhibitors that are not specific to M^{Pro} , while chloroquine, oxytetracycline, montelukast, candesartan, and dipyrindamole do not inhibit M^{Pro} in any of the assays tested. Overall, our study highlights the need of stringent hit validation at the early stage of drug discovery.

© 2022 Chinese Pharmaceutical Association and Institute of Materia Medica, Chinese Academy of Medical Sciences. Production and hosting by Elsevier B.V. This is an open access article under the CC BY-NC-ND license (<http://creativecommons.org/licenses/by-nc-nd/4.0/>).

Abbreviations: M^{Pro} , Main protease; PL^{Pro} , Papain-like protease; FFluc, Firefly luciferase; Rluc, *Renilla* luciferase.

*Corresponding author.

E-mail address: junwang@pharmacy.arizona.edu (Jun Wang).

Peer review under responsibility of Chinese Pharmaceutical Association and Institute of Materia Medica, Chinese Academy of Medical Sciences

<https://doi.org/10.1016/j.apsb.2021.10.026>

2211-3835 © 2022 Chinese Pharmaceutical Association and Institute of Materia Medica, Chinese Academy of Medical Sciences. Production and hosting by Elsevier B.V. This is an open access article under the CC BY-NC-ND license (<http://creativecommons.org/licenses/by-nc-nd/4.0/>).

1. Introduction

SARS-CoV-2 is the causative agent for COVID-19, which infected 229 million people and led to 4.71 million deaths as of September 23, 2021. SARS-CoV-2 is the third coronavirus that causes epidemics and pandemics in human. SARS-CoV-2, along with SARS-CoV and MERS-CoV, belong to the β genera of the coronaviridae family¹. SARS-CoV-2 encodes two viral cysteine proteases, the main protease (M^{pro}) and the papain-like protease (PL^{pro}), that mediate the cleavage of viral polyproteins pp1a and pp1ab during viral replication^{2–4}. M^{pro} cleaves at more than 11 sites at the viral polyproteins and has a high substrate preference for glutamine at the P1 site⁵. In addition, the M^{pro} is highly conserved among coronaviruses that infect human including SARS-CoV-2, SARS-CoV, MERS-CoV, HCoV-OC43, HCoV-NL63, HCoV-229E, and HCoV-HKU1. For these reasons, M^{pro} becomes a high-profile drug target for the development of broad-spectrum antivirals. Structurally disparate compounds including FDA-approved drugs and bioactive compounds have been reported as M^{pro} inhibitors^{6–10}, several of which also have *in vivo* antiviral efficacy against SARS-CoV-2^{11–15}.

FRET assay is the gold standard assay for protease and is typically used as a primary assay for the screening of M^{pro} inhibitors. However, the FRET assay conditions used by different groups vary significantly in terms of the protein and substrate concentrations, pH, reducing reagent, and detergent. Reducing reagent is typically added in the assay buffer to prevent the non-specific oxidation or alkylation of the catalytic C145 in M^{pro}. Nonetheless, many studies do not include reducing reagents in the FRET assay buffer, leading to debatable results¹⁶. Regardless of the assay condition, FRET assay is a cell free biochemical assay, which does not mimic the cellular environment; therefore, the results cannot be used to accurately predict the cellular activity of the M^{pro} inhibitor or the antiviral activity. Moreover, one limiting factor for M^{pro} inhibitor development is that the cellular activity has to be tested against infectious SARS-CoV-2 in BSL-3 facility, which is inaccessible to many researchers. For these reasons, there is a pressing need of secondary M^{pro} target-specific assays that can closely mimic the cellular environment and be used to rule out false positives.

In this study, we report our findings of validating or invalidating the literature reported M^{pro} inhibitors using the cell lysate Protease-Glo luciferase assay and the cell-based FlipGFP assay, in conjunction to the cell-free FRET assay and thermal shift-binding assay. The purpose is to elucidate their target specificity and cellular target engagement. The Protease-Glo luciferase assay was developed in this study, and the FlipGFP assay was recently developed by us and others^{17–20}. Our results have collectively shown that majority of the M^{pro} inhibitors identified from drug repurposing screening including ebiselen, carmofur, disulfiram, and shikonin are promiscuous cysteine inhibitors that are not specific to M^{pro}, while chloroquine, oxytetracycline, montelukast, candesartan, and dipyrindamole do not inhibit M^{pro} in any of the assays tested. The results presented herein highlight the pressing need of stringent hit validation at the early stage of drug discovery to minimize the catastrophic failure in the following translational development.

2. Methods and materials

2.1. Protein expression and purification

The tag-free SARS CoV-2 M^{pro} protein with native N- and C-termini was expressed in pSUMO construct as described previously³.

2.2. Enzymatic assays

The FRET-based protease was performed as described previously². Briefly, 100 nmol/L of M^{pro} protein in the reaction buffer containing 20 mmol/L HEPES, pH 6.5, 120 mmol/L NaCl, 0.4 mmol/L EDTA, 4 mmol/L DTT, and 20% glycerol was incubated with serial concentrations of the testing compounds at 30 °C for 30 min. The proteolytic reactions were initiated by adding 10 μ mol/L of FRET-peptide substrate [Dabcyl-KTSAVLQ/SGFRKME (Edans)] and recorded in Cytation 5 imaging reader (Thermo Fisher Scientific) with 360/460 filter cube for 1 h. The proteolytic reaction initial velocity in the presence or absence of testing compounds was determined by linear regression using the data points from the first 15 min of the kinetic progress curves. IC₅₀ values were calculated by a 4-parameter dose–response function in Prism 8.

2.3. Thermal shift assay (TSA)

Direct binding of testing compounds to SARS CoV-2 M^{pro} protein was evaluated by differential scanning fluorimetry (DSF) using a Thermal Fisher QuantStudio 5 Real-Time PCR System as previously described². Briefly, SARS CoV-2 M^{pro} protein was diluted into reaction buffer to a final concentration of 3 μ mol/L and incubated with 40 μ mol/L of testing compounds at 30 °C for 30 min. DMSO was included as a reference. SYPRO orange (1 \times , Thermal Fisher, catalog No. S6650) was added, and the fluorescence signal was recorded under a temperature gradient ranging from 20 to 95 °C with incremental step of 0.05 °C/s. The melting temperature (T_m) was calculated as the mid log of the transition phase from the native to the denatured protein using a Boltzmann model in Protein Thermal Shift Software v1.3. ΔT_m was the difference between T_m in the presence of testing compounds and T_m in the presence of DMSO.

2.4. FlipGFP M^{pro} assay

The construction of FlipGFP-M^{pro} plasmid was described previously¹⁷. The assay was carried out as follows: 293T cells were seeded in 96-well black, clear bottomed Greiner plate (catalog No. 655090) and incubated overnight to reach 70%–90% confluency. 50 ng of FlipGFP-M^{pro} plasmid and 50 ng SARS CoV-2 M^{pro} expression plasmid pcDNA3.1 SARSCoV-2 M^{pro} were transfected into each well with transfection reagent TransIT-293 (Mirus catalog No. MIR 2700) according to the manufacturer's protocol. Three hours after transfection, 1 μ L of testing compound was directly added to each well without medium change. Two days after transfection, images were taken with Cytation 5 imaging reader (Biotek) using GFP and mCherry channels *via* 10 \times objective lens and were analyzed with Gen5 3.10 software (Biotek). The mCherry signal alone in the presence of testing compounds was utilized to evaluate the compound cytotoxicity.

2.5. Protease-Glo luciferase assay

pGloSensor-30F DEVD vector was obtained from Promega (Catalog No. CS182101). pGloSensor-30F M^{pro} plasmid was generated by replacing the original caspase cutting sequence (DEVDG) with SARS CoV-2 M^{pro} cutting sequence (AVLQ/SGFR) from BamHI/HindIII sites. The DNA duplex containing M^{pro} cutting sequence was generated by annealing two

5'-phosphoriated primers: forward: GATCCGCCGTGCGCA-GAGCGGCTTTCAGA; and reverse: AGCTTCTGAAGCCGCTCTGCAGCACGGCG. Protease-Glo luciferase assay was carried out as follows: 293T cells in 10 cm culture dish were transfected with pGloSensor-30F M^{Pro} plasmid in the presence of transfection reagent TransIT-293 (Mirus catalog No. MIR 2700) according to the manufacturer's protocol. 24 h after transfection, cells were washed with PBS once, then each dish of cells was lysed with 5 mL of PBS+ 1% Triton-X100; cell debris was removed by centrifuge at 2000 × *g* for 10 min. Cell lysates was freshly frozen to −80 °C until ready to use. During the assay, 20 μL cell lysate was added to each well in 96-well flat bottom white plate (Fisherbrand Catalog No. 12566619), then 1 μL of testing compound or DMSO was added to each well and mixed at room temperature for 5 min. 5 μL of 200 nmol/L *Escherichia coli* expressed SARS CoV-2 M^{Pro} protein was added to each well to initiate the proteolytic reaction (the final M^{Pro} protein concentration is around 40 nmol/L). The reaction mix was further incubated at 30 °C for 30 min. The firefly and *Renilla* luciferase activity were determined with Dual-Glo Luciferase Assay according to manufacturer's protocol (Promega Catalog No. E2920). The efficacy of testing compounds against M^{Pro} was evaluated by plotting the ratio of firefly luminescence signal over the *Renilla* luminescence signal versus the testing compound concentrations with a 4-parameter dose–response function in Prism 8.

2.6. Antiviral assay in Calu-3 cells

The antiviral assay was performed as previously described²¹. Calu-3 cells (ATCC, HTB-55) were plated in 384 well plates and grown in minimal Eagle's medium supplemented with 1% non-essential amino acids, 1% penicillin/streptomycin, and 10% FBS. The next day, 50 nL of compound in DMSO was added as an 8-pt dose response with three-fold dilutions between testing concentrations in triplicate, starting at 40 μmol/L final concentration. The negative control (DMSO, *n* = 32) and positive control (10 μmol/L remdesivir, *n* = 32) were included on each

assay plate. Calu-3 cells were pretreated with controls and testing compounds (in triplicate) for 2 h prior to infection. In BSL-3 containment, SARS-CoV-2 (isolate USA-WA1/2020) diluted in serum free growth medium was added to plates to achieve an MOI of 0.5. Cells were incubated with compounds and SARS-CoV-2 virus for 48 h. Cells were fixed and then immunostained with anti-dsRNA (J2) and nuclei were counterstained with Hoechst 33342 for automated microscopy. Automated image analysis quantifies the number of cells per well (toxicity) and the percentage of infected cells (dsRNA + cells/cell number) per well. SARS-CoV-2 infection at each drug concentration was normalized to aggregated DMSO plate control wells and expressed as percentage-of-control:

$$\text{POC} = \% \text{ Infection}_{\text{sample}} / \text{Avg} \% \text{ Infection}_{\text{DMSO cont}} \quad (1)$$

A non-linear regression curve fit analysis (GraphPad Prism 8) of POC Infection and cell viability versus the log₁₀ transformed concentration values to calculate EC₅₀ values for Infection and CC₅₀ values for cell viability. Selectivity index (SI) was calculated as a ratio of drug's CC₅₀ and EC₅₀ values:

$$\text{SI} = \text{CC}_{50} / \text{EC}_{50} \quad (2)$$

3. Results and discussion

3.1. Assay validation using GC-376 and rupintrivir as positive and negative controls

The advantages and disadvantages of the cell lysate Protease-Glo luciferase assay and the cell-based FlipGFP assay compared to the cell free FRET assay are listed in Table 1. To minimize the bias from a particular assay, we apply all these three functional assays together with the thermal shift-binding assay for the hit validation.

In the cell-based FlipGFP assay, the cells were transfected with two plasmids, one expresses the SARS-CoV-2 M^{Pro}, and another

Table 1 Advantages and disadvantages of the three functional assays used in this study.

Assay	Advantage	Disadvantage
FRET assay	<ul style="list-style-type: none"> • High throughput 	<ul style="list-style-type: none"> • Compounds that quench the fluorophore will show up as false positives • Assay interference from fluorescent compounds, detergents, and aggregators. • Cannot be used to predict the cellular antiviral activity • No standard condition among scientific community
FlipGFP assay	<ul style="list-style-type: none"> • Can rule out compounds that are cytotoxic, membrane impermeable, or substrates of drug efflux pump • A close mimetic of virus-infected cell • Can be used to predict the cellular antiviral activity • Reveals cellular target engagement 	<ul style="list-style-type: none"> • The assay takes 48 h, thus it cannot be used for cytotoxic compounds • Interference from fluorescent compounds • Not high throughput
Protease-Glo luciferase assay	<ul style="list-style-type: none"> • High throughput • Reveals cellular target engagement • Can be used to test cytotoxic compounds 	<ul style="list-style-type: none"> • Cannot be used to predict the cellular antiviral activity

expresses the GFP reporter²². The GFP reporter plasmid expresses three proteins including the GFP β 10– β 11 fragment flanked by the K5/E5 coiled coil, the GFP β 1–9 template, and the mCherry (Fig. 1A). mCherry serves as an internal control for the normalization of the expression level or the quantification of compound toxicity. In the assay design, β 10 and β 11 were conformationally constrained in the parallel position by the heterodimerizing K5/E5 coiled coil with a M^{pro} cleavage sequence (AVLQ↓SGFR). Upon cleavage of the linker by M^{pro}, β 10 and β 11 become antiparallel and can associate with the β 1–9 template, resulting in the restoration of the GFP signal. In principle, the ratio of GFP/mCherry fluorescence is proportional to the enzymatic activity of M^{pro}. The

FlipGFP M^{pro} assay has been used by several groups to characterize the cellular activity of M^{pro} inhibitors^{17,19,20}.

In the cell lysate Protease-Glo luciferase assay, the cells were transfected with pGloSensor-30F luciferase reporter (Fig. 1B)²³. The pGloSensor-30F luciferase reporter plasmid expresses two proteins, the inactive, circularly permuted firefly luciferase (FFluc) and the active *Renilla* luciferase (Rluc). *Renilla* luciferase was included as an internal control to normalize the protein expression level. The firefly luciferase was split into two fragments, the FF 4–354 and FF 358–544. The SARS-CoV-2 M^{pro} substrate cleavage sequence (AVLQ/SGFR) was inserted in between the two fragments. Before protease cleavage, the

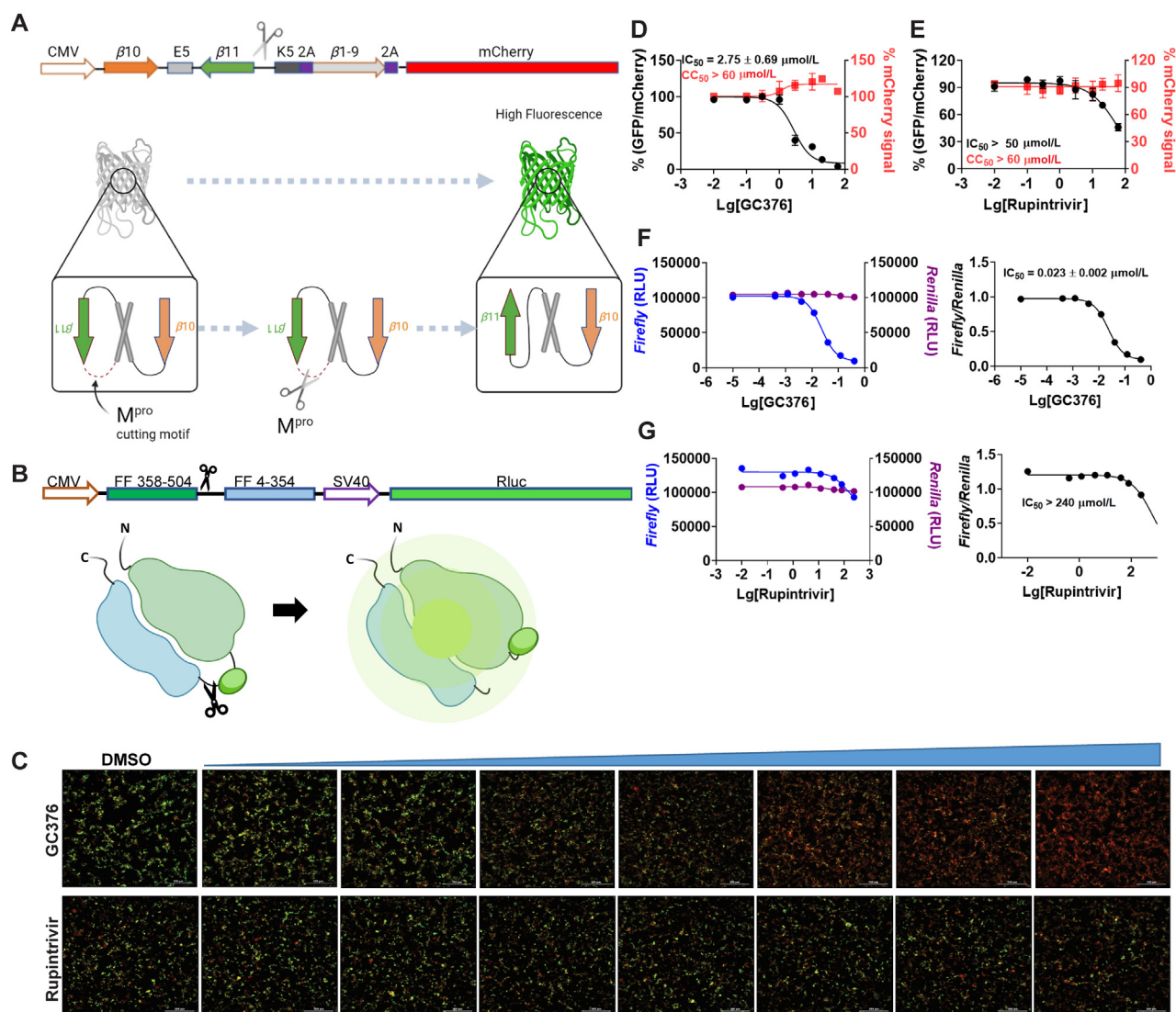
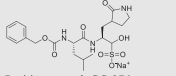
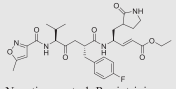
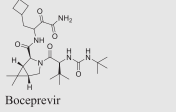
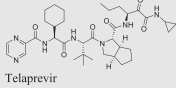
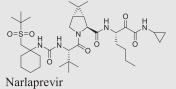
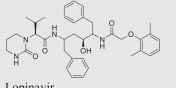
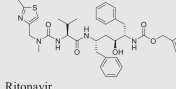
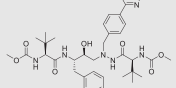
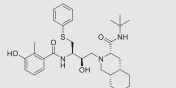
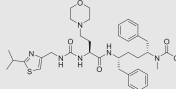
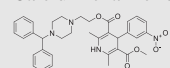


Figure 1 Principles for the FlipGFP and Protease-Glo luciferase assays and assay validation with control compounds. (A) Assay principle for the FlipGFP assay. Diagram of the FlipGFP M^{pro} reporter plasmid is shown. (B) Assay principle for the Protease-Glo luciferase assay. Diagram of pGlo-M^{pro} luciferase reporter in the pGloSensor-30F vector is shown. (C) Representative images from the FlipGFP-M^{pro} assay. Dose-dependent decrease of GFP signal was observed with the increasing concentration of GC-376 (positive control); almost no GFP signal change was observed with the increasing concentration of rupintrivir (negative control). The scale bar is 300 μ m. (D) and (E) Dose–response curve of the ratio of GFP/mCherry fluorescence with GC-376 and rupintrivir; mCherry signal alone was used to normalize protein expression level or calculate compound cytotoxicity. (F)–(G) Protease-Glo luciferase assay results of GC-376 and rupintrivir. Left column showed *Firefly* and *Renilla* luminescence signals in the presences of increasing concentrations of GC-376 and rupintrivir; Right column showed dose–response curve plots of the ratio of FFluc/Rluc luminescence. The results are mean \pm standard deviation from three repeats. Compound concentration, μ mol/L.

Table 2 Summary of results.

Compd.	FRET IC ₅₀ (μmol/L)	TSA ΔT _m (°C)	FlipGFP IC ₅₀ (μmol/L)	pGlo-M ^{pro} luciferase (μmol/L)	Anti-viral (μmol/L) Vero CPE	PDB code	Comment
Control compounds							
 Positive control: GC-376	0.030 ± 0.008 0.15 ± 0.03 ²⁵ 0.052 ± 0.007 ²⁶	18.30 ²	2.75 ± 1.06	0.023 ± 0.002	3.37 ± 1.68 ² 0.70 ²⁵ 10 ± 4.2 ²⁶	6WTT ² 6WTJ ²⁷ 7C6U ²⁵	Positive control
 Negative control: Rupintrivir	>20 ² >100 ⁸	0.01	>50	>240	(Nluc)1.87 ± 0.47 ²⁴	N.A.	Negative control
HCV protease inhibitors							
 Boceprevir	4.13 ± 0.61 ² 2.9 ± 0.6 ²⁸ 8.0 ± 1.5 ²⁵ 3.1 ²⁹ 3.7 ± 1.7 ³⁰	6.67 ²	18.33 ± 3.54	4.49 ± 1.42	1.31 ± 0.58 ² 19.6 ²⁸ 15.57 ²⁵ >50 ³⁰ 5.4 (293T) ²⁸	6XQU ²⁹ 7C6S ²⁵ 7COM ³¹	Validated M ^{pro} inhibitor
 Telaprevir	24.2 ± 6.1 18.7 ± 6.4 ²⁸ 18 ²⁹ 17.9 ± 4.5 ³⁰	1.03	19.9 ± 3.0	41.91 ± 6.82	>50 ²⁸ 20.5 (293T) ²⁸	6XQS ²⁹ 7C7P ³¹ 7LB7 ³²	Validated M ^{pro} inhibitor
 Narlaprevir	5.73 ± 0.67 ² 2.2 ± 0.4 ²⁸ 5.1 ²⁹	5.18 ²	23.8 ± 6.5	10.99 ± 1.96	7.7 ² 15 (293T) ²⁸	6XQT ²⁹ 7D1O ³³	Validated M ^{pro} inhibitor
HIV protease inhibitors							
 Lopinavir	>60 ² 234 ± 98 ³⁰	-0.60	>20	>240	(Nluc)9.00 ± 0.42 ²⁴ 19 ± 8 ³⁴ 25 ³⁵	N.A.	Not a M ^{pro} inhibitor
 Ritonavir	>20 ² >1000 ³⁰	-0.65	>20	>240	> 100 ³⁵	N.A.	Not a M ^{pro} inhibitor
 Atazanavir	>60 ³⁶ 7.5 ± 0.3 ³⁷	0.19	>60	>240	2.0 ± 0.12 ³⁸	N.A.	Not a M ^{pro} inhibitor
 Nelfinavir	>20 ² 118 ± 18 ³⁰	-0.60	>10	>240	3.3 ³⁰ (Nluc)0.77 ± 0.32 ²⁴ 3.1 ± 0.06 ³⁴	N.A.	Not a M ^{pro} inhibitor
 Cobicistat	>20 6.7 ± 0.6 ³⁹	-0.65	>20	>240	(Nluc)2.74 ± 0.20 ²⁴	N.A.	Not a M ^{pro} inhibitor

Calcium channel blocker



64.2 ± 9.8
4.81 ± 1.87⁴⁰

0.45

>10

>240

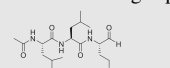
N.A.

N.A.

Not a M^{pro} inhibitor

Manidipine

Hits from drug repurposing



0.97 ± 0.27²
8.98 ± 2.0²⁶

6.65²

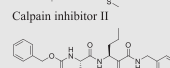
>60

0.60 ± 0.11

2.07 ± 0.76²
27 ± 1.4²⁶

6XA4³

Validated M^{pro}
Inhibitor
Cell-type dependent



0.45 ± 0.06²
6.48 ± 3.4²⁶

7.86²

38.71 ± 5.66

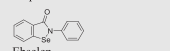
0.79 ± 0.10

0.49 ± 0.18²
1.3 ± 0.57²⁶

6XBH³

Validated M^{pro}
Inhibitor
Cell-type dependent

Calpain inhibitor XII



>60⁴¹
0.67 ± 0.09^{16,42}
>100²⁶

0.14⁴¹

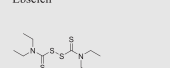
>60

>60

4.67 ± 0.80^{16,42}
>100²⁶

7BAK⁴²Not a M^{pro} inhibitor

Ebselelen



>60⁴¹
9.35 ± 0.18¹⁶

0.21⁴¹

>60

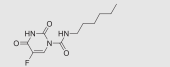
>240

not active¹⁶

N.A.

Not a M^{pro} inhibitor

Disulfiram



28.2 ± 9.5⁴¹
1.82 ± 0.06¹⁶
>100²⁶

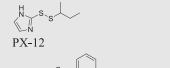
0.35⁴¹

>60

>240

>100²⁶7BUY⁴³Not a M^{pro} inhibitor

Carmofur



>60⁴¹
21.39 ± 7.06¹⁶

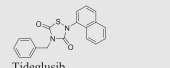
-0.14⁴¹

>60

>240

not active¹⁶

N.A.

Not a M^{pro} inhibitor

>60⁴¹
1.55 ± 0.30¹⁶

-0.21⁴¹

>60

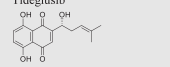
>240

not active¹⁶

N.A.

Not a M^{pro} inhibitor

Tideglusib



>60⁴¹
15.75 ± 8.22¹⁶
15.0 ± 3.0²⁶

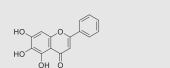
0.40⁴¹

>20

>240

>100²⁶7CA8⁴⁴Not a M^{pro} inhibitor

Shikonin



>60
0.39 ± 0.11⁴⁵
0.94 ± 0.20⁴⁶

0.21

>60

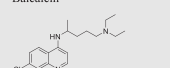
>240

2.92 ± 0.06⁴⁵
2.94 ± 1.19⁴⁶

N.A.

Not a M^{pro} inhibitor

Baicalein



>200³⁶
3.9 ± 0.2³⁷

0.09³⁶

>200

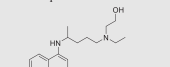
>800

1.13⁴⁷

N.A.

Not a M^{pro} inhibitor

Chloroquine



>200³⁶
2.9 ± 0.3³⁷

0.16³⁶

>200

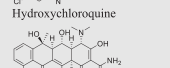
>800

2.71 to 7.36⁴⁸

N.A.

Not a M^{pro} inhibitor

Hydroxychloroquine



>60³⁶
15.2 ± 0.9³⁷

0.16³⁶

>60

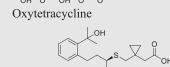
>240

N.A.

N.A.

Not a M^{pro} inhibitor

Oxytetracycline



13.5 ± 1.0³⁶
7.3 ± 0.5³⁷

-0.68³⁶

>60

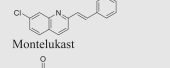
>240

N.A.

N.A.

Not a M^{pro} inhibitor

Montelukast



>60³⁶
K_i = 0.62 ± 0.05³⁷

0.23³⁶

>60

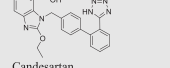
>240

N.A.

N.A.

Not a M^{pro} inhibitor

Candesartan



29.4 ± 3.2³⁶
0.60 ± 0.01³⁷

-0.19³⁶

>60

>240

N.A.

N.A.

Not a M^{pro} inhibitor

Dipyridamole

N.A., not available.

pGloSensor-30F reporter comprises an inactive circularly permuted firefly luciferase. The cells were lysed at 24 h post transfection, and M^{PRO} and the luciferase substrates were added to initiate the reaction. Upon protease cleavage, a conformational change in firefly luciferase leads to drastically increase in luminescence. In principle, the ratio of FFluc/RLuc luminescence is proportional to the enzymatic activity of M^{PRO}.

To calibrate the FlipGFP and Protease-Glo luciferase assays, we chose GC-376 and rupintrivir as positive and negative controls, respectively. The IC₅₀ values for GC-376 in the FlipGFP and Protease-Glo luciferase assays were 2.75 and 0.023 μmol/L, respectively (Fig. 1C, D, and F). The IC₅₀ value in the FlipGFP assay is similar to its antiviral activity (Table 2), suggesting the FlipGFP can be used to predict the cellular antiviral activity. In contrast, rupintrivir showed no activity in either the FlipGFP (IC₅₀ > 50 μmol/L) (Fig. 1C second row and 1E) or the Protease-Glo luciferase assay (IC₅₀ > 100 μmol/L) (Fig. 1G), which agrees with the lack of inhibition from the FRET assay (IC₅₀ > 20 μmol/L). Nonetheless, rupintrivir was reported to inhibit SARS-CoV-2 replication with an EC₅₀ of 1.87 μmol/L using the nanoluciferase SARS-CoV-2 reporter virus (SARS-CoV-2-Nluc) in A549-hACE2 cells²⁴ (Table 2). The discrepancy indicates that the mechanism of action of rupintrivir might be independent of M^{PRO} inhibition. Overall, the FlipGFP and Protease-Glo luciferase assays are validated as target-specific assays for SARS-CoV-2 M^{PRO}.

3.2. HCV protease inhibitors

The HCV protease inhibitors have been proven a rich source of SARS-CoV-2 M^{PRO} inhibitors^{2,28,29}. From screening a focused protease library using the FRET assay, we discovered simeprevir, boceprevir, and naldaprevir as SARS-CoV-2 M^{PRO} inhibitors with IC₅₀ values of 13.74, 4.13, and 5.73 μmol/L, respectively, while telaprevir was less active (31% inhibition at 20 μmol/L)². The binding of boceprevir to M^{PRO} was characterized by thermal shift assay and native mass spectrometry. Boceprevir inhibited SARS-CoV-2 viral replication in Vero E6 cells with EC₅₀ values of 1.31 and 1.95 μmol/L in the primary CPE and secondary viral yield reduction assays, respectively (Table 2). In parallel, Fu et al.²⁵ also reported boceprevir as a SARS-CoV-2 M^{PRO} inhibitor with an enzymatic inhibition IC₅₀ of 8.0 μmol/L and an antiviral EC₅₀ of 15.57 μmol/L. The X-ray crystal structure of M^{PRO} with boceprevir was solved, revealing a covalent modification of the C145 thiol by the ketoamide (PDBs: 6XQU²⁹, 7C6S²⁵, 7COM³¹).

In the current study, we found that boceprevir showed moderate inhibition in the cellular FlipGFP M^{PRO} assay with an IC₅₀ of 18.33 μmol/L (Fig. 2A and B), a more than 4-fold increase compared to the IC₅₀ in the FRET assay (4.13 μmol/L). The IC₅₀ value of boceprevir in the cell lysate Protease-Glo luciferase assay was 4.49 μmol/L (Fig. 2E). In comparison, telaprevir and naldaprevir showed weaker inhibition than boceprevir in both the FlipGFP and Protease-Glo luciferase assays (Fig. 2A, C, D, F, and G), which is consistent with their weaker potency in the FRET assay (Table 2). Overall, boceprevir, telaprevir, and naldaprevir have been validated as SARS-CoV-2 M^{PRO} inhibitors in both the cellular FlipGFP assay and the cell lysate Protease-Glo luciferase assay. Therefore, the antiviral activity of these three compounds against SARS-CoV-2 are likely due to M^{PRO} inhibition. Although the inhibition of M^{PRO} by boceprevir is relatively weak compared to GC-376, several highly potent M^{PRO} inhibitors were subsequently designed as hybrids of boceprevir and GC-376^{11,17,31}

including the Pfizer oral drug candidate PF-07321332, which contain the dimethylcyclopropylproline at the P2 substitution.

3.3. HIV protease inhibitors

HIV protease inhibitors, especially Kaletra, have been hotly pursued as potential COVID-19 treatment at the beginning of the pandemic. Kaletra was first tested in clinical trial during the SARS-CoV outbreak in 2003 and showed somewhat promising results based on the limited data⁴⁹. However, a double-blinded, randomized trial concluded that Kaletra was not effective in treating severe COVID-19^{50,51}. In SARS-CoV-2 infection ferret models, Kaletra showed marginal effect in reducing clinical symptoms, while had no effect on virus titers⁵².

Kaletra is a combination of lopinavir and ritonavir. Lopinavir is a HIV protease inhibitor, and ritonavir is used as a booster. Ritonavir does not inhibit the HIV protease and it is a cytochrome P450-3A4 inhibitor⁵³. When used in combination, ritonavir can enhance other protease inhibitors by preventing or slowing down the metabolism. In cell culture, lopinavir was reported to inhibit the nanoluciferase SARS-CoV-2 reporter virus with an EC₅₀ of 9 μmol/L²⁴. In two other studies, lopinavir showed moderate antiviral activity against SARS-CoV-2 activity with EC₅₀ values of 19 ± 8 μmol/L³⁴ and 25 μmol/L³⁵. As such, it was assumed that lopinavir inhibited SARS-CoV-2 through inhibiting the M^{PRO}. However, lopinavir showed no activity against SARS-CoV-2 M^{PRO} in the FRET assay from our previous study (IC₅₀ > 60 μmol/L)². Wu et al.⁵⁴ also showed that lopinavir was a weak inhibitor against SARS-CoV M^{PRO} with an IC₅₀ of 50 μmol/L. In the current study, we further confirmed the lack of binding of lopinavir to SARS-CoV-2 M^{PRO} in the thermal shift assay (ΔT_m = -0.60 °C, Table 2). The result from the FlipGFP assay was not conclusive as lopinavir was cytotoxic. Lopinavir was not active in the Protease-Glo luciferase assay. Taken together, lopinavir is not a M^{PRO} inhibitor.

Ritonavir was not active in both the FlipGFP M^{PRO} and the Protease-Glo luciferase assays, which is consistent with the lack of activity in the FRET assay and the thermal shift binding assay (Table 2). Therefore, ritonavir is not a M^{PRO} inhibitor.

We also tested additional HIV antivirals including atazanavir, nelfinavir, and cobicistat. Atazanavir and nelfinavir were reported as a potent SARS-CoV-2 antiviral with EC₅₀ values of 2.0 ± 0.12³⁸ and 0.77 μmol/L²⁴ using the infectious SARS-CoV-2 and the nanoluciferase reporter virus (SARS-CoV-2-Nluc), respectively. A drug repurposing screening similar identified nelfinavir as a SARS-CoV-2 antiviral with an IC₅₀ of 3.3 μmol/L³⁰. Gupta et al.³⁹ showed that cobicistat inhibited M^{PRO} with an IC₅₀ of 6.7 μmol/L in the FRET assay. Cobicistat was also reported to have antiviral activity against SARS-CoV-2 with an EC₅₀ of 2.74 ± 0.20 μmol/L using the SARS-CoV-2-Nluc reporter virus²⁴. However, our FRET assay showed that nelfinavir and cobicistat did not inhibit M^{PRO} in the FRET assay (IC₅₀ > 20 μmol/L), which was further confirmed by the lack of binding to M^{PRO} in the thermal shift assay (Table 2). The results of atazanavir, nelfinavir, and cobicistat from the FlipGFP assay were not conclusive due to compound cytotoxicity (Fig. 3A–F). None of the compounds showed inhibition in the Protease-Glo luciferase assay (Fig. 3G–K).

Collectively, our results have shown that the HIV protease inhibitors including lopinavir, ritonavir, atazanavir, nelfinavir, and cobicistat are not M^{PRO} inhibitors. Nonetheless, given the potent antiviral activity of lopinavir, atazanavir, nelfinavir, and cobicistat

against SARS-CoV-2, it might worth to conduct resistance selection to elucidate their drug target(s).

3.4. Bioactive compounds from drug repurposing

Several bioactive compounds have been identified as SARS-CoV-2 M^{PRO} inhibitors through either virtual screening or FRET-based HTS. We are interested in validating these hits using the FlipGFP and the Protease-Glo luciferase assays.

Manidipine was identified as a SARS-CoV-2 M^{PRO} inhibitor from a virtual screening and was subsequently shown to inhibit M^{PRO} with

an IC₅₀ of 4.81 μmol/L in the FRET assay⁴⁰. No antiviral data was provided. When we repeated the FRET assay, the IC₅₀ was 64.2 μmol/L (Table 2). Manidipine also did not show binding to M^{PRO} in the thermal shift assay. Furthermore, manidipine showed no activity in either the FlipGFP assay or the Protease-Glo luciferase assay (Fig. 4A, B, and F). Therefore, our results invalidated manidipine as a SARS-CoV-2 M^{PRO} inhibitor. A recent study independently confirmed our results and suggested that manidipine might form colloidal aggregates⁵⁵, leading to inactivation of M^{PRO}. In the presence of 0.05% Tween-20, manidipine was not active against M^{PRO} in the FRET assay (IC₅₀ > 100 μmol/L).

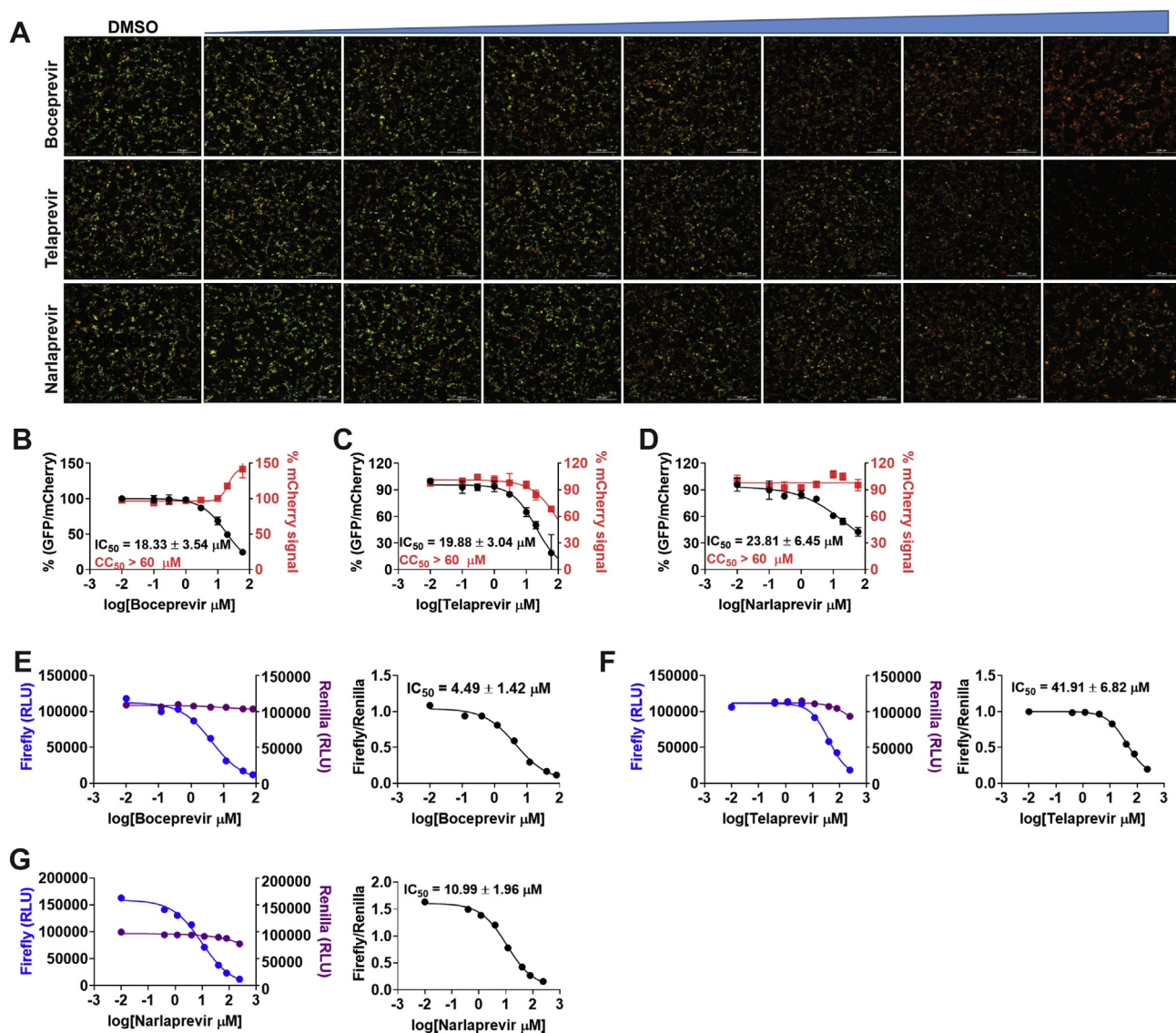


Figure 2 Validation/invalidation of hepatitis C virus NS3/4A protease inhibitors boceprevir, telaprevir, and narlaprevir as SARS CoV-2 M^{PRO} inhibitors using the FlipGFP assay and Protease-Glo luciferase assay. (A) Representative images from the FlipGFP-M^{PRO} assay. Dose-dependent decrease of GFP signal was observed with the increasing concentration of boceprevir, telaprevir or narlaprevir. The scale bar is 300 μm. (B)–(D) Dose–response curve of the GFP and mCherry fluorescent signals for boceprevir (B), telaprevir (C) or narlaprevir (D); mCherry signal alone was used to normalize protein expression level or calculate compound toxicity. (E)–(G) Protease-Glo luciferase assay results of boceprevir (E), telaprevir (F) or narlaprevir (G). Left column shows *Firefly* and *Renilla* luminescence signals in the presences of increasing concentrations of boceprevir, telaprevir or narlaprevir; Right column shows dose–response curve plots of the ratio of FFluc/Rlu luminescence. *Renilla* luminescence signal alone was used to normalize protein expression level. The results are mean ± standard deviation from three repeats. Compound concentration, μmol/L.

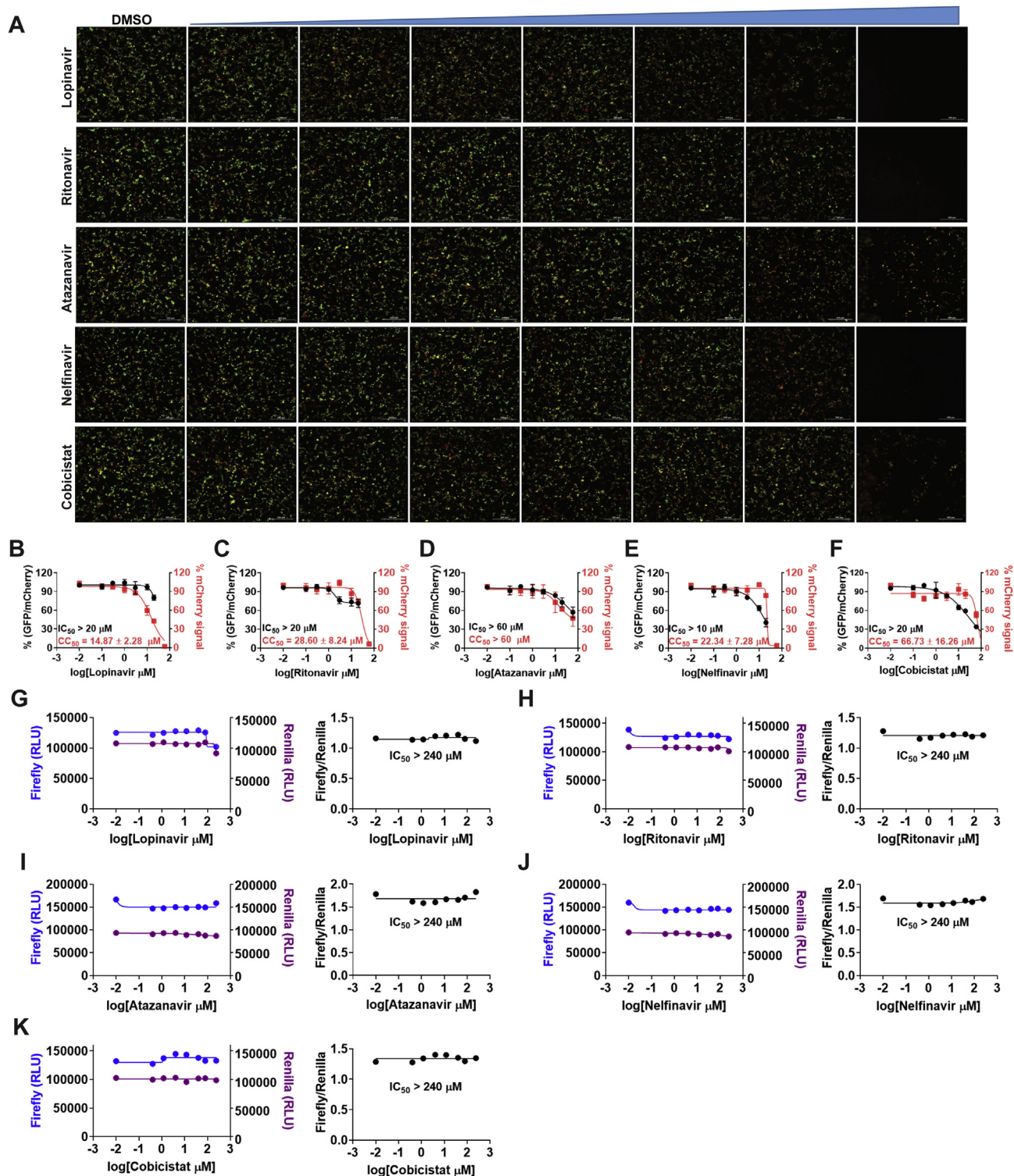


Figure 3 Validation/invalidation of HIV protease inhibitors lopinavir, ritonavir, atazanavir, nelfinavir, and cobicistat as SARS CoV-2 M^{Pro} inhibitors using the FlipGFP assay and Protease-Glo luciferase assay. (A) Representative images from the FlipGFP-M^{Pro} assay. The scale bar is 300 μm . (B)–(F) Dose–response curve of the GFP and mCherry fluorescent signals for lopinavir (B), ritonavir (C), atazanavir (D), nelfinavir (E), and cobicistat (F); mCherry signal alone was used to normalize protein expression level or calculate compound cytotoxicity. (G)–(K) Protease-Glo luciferase assay results of lopinavir (G), ritonavir (H), atazanavir (I), nelfinavir (J), and cobicistat (K). Left column shows *Firefly* and *Renilla* luminescence signals in the presences of increasing concentrations of lopinavir, ritonavir, atazanavir, nelfinavir, and cobicistat; Right column shows dose–response curve plots of ratio of FFluc/RLuc luminescence. *Renilla* luminescence signal alone was used to normalize protein expression level. None of the compounds shows significant inhibition in the presence of up to 240 $\mu\text{mol/L}$ compounds. The results are mean \pm standard deviation from three repeats. Compound concentration, $\mu\text{mol/L}$.

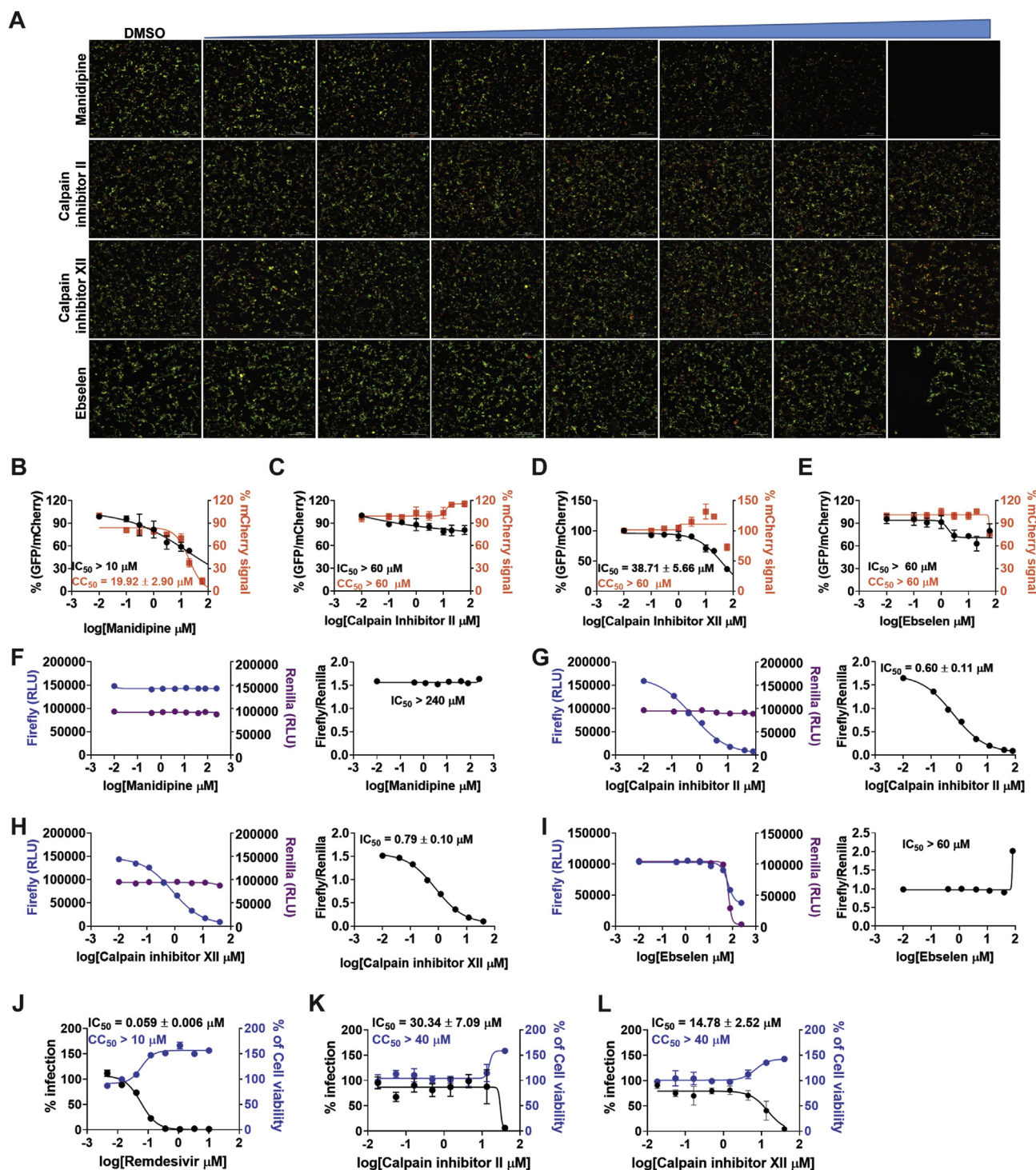


Figure 4 Validation/invalidation of manidipine, calpain inhibitors II and XII, and ebselen as SARS CoV-2 M^{PRO} inhibitors using the FlipGFP assay and Protease-Glo luciferase assay. (A) Representative images from the FlipGFP-M^{PRO} assay. The scale bar is 300 μ m. (B)–(E) Dose–response curve of the GFP and mCherry fluorescent signals for manidipine (B), calpain inhibitor II (C), calpain inhibitor XII (D), and ebselen (E); mCherry signal alone was used to normalize protein expression level or calculate compound cytotoxicity. (F)–(I) Protease-Glo luciferase assay results of manidipine (F), calpain inhibitor II (G), calpain inhibitor XII (H), and ebselen (I). Left column shows *Firefly* and *Renilla* luminescence signals in the presences of increasing concentrations of lopinavir, ritonavir, atazanavir, nelfinavir, and cobicistat; Right column shows dose–response curve plots of the ratio of FFluc/RLuc luminescence. *Renilla* luminescence signal alone was used to normalize protein expression level. (J)–(K) Antiviral activity of remdesivir (J), calpain inhibitor II (K), and calpain inhibitor XII (L) against SARS-CoV-2 in Calu-3 cells. The results are mean \pm standard deviation from three repeats. Compound concentration, μ mol/L.

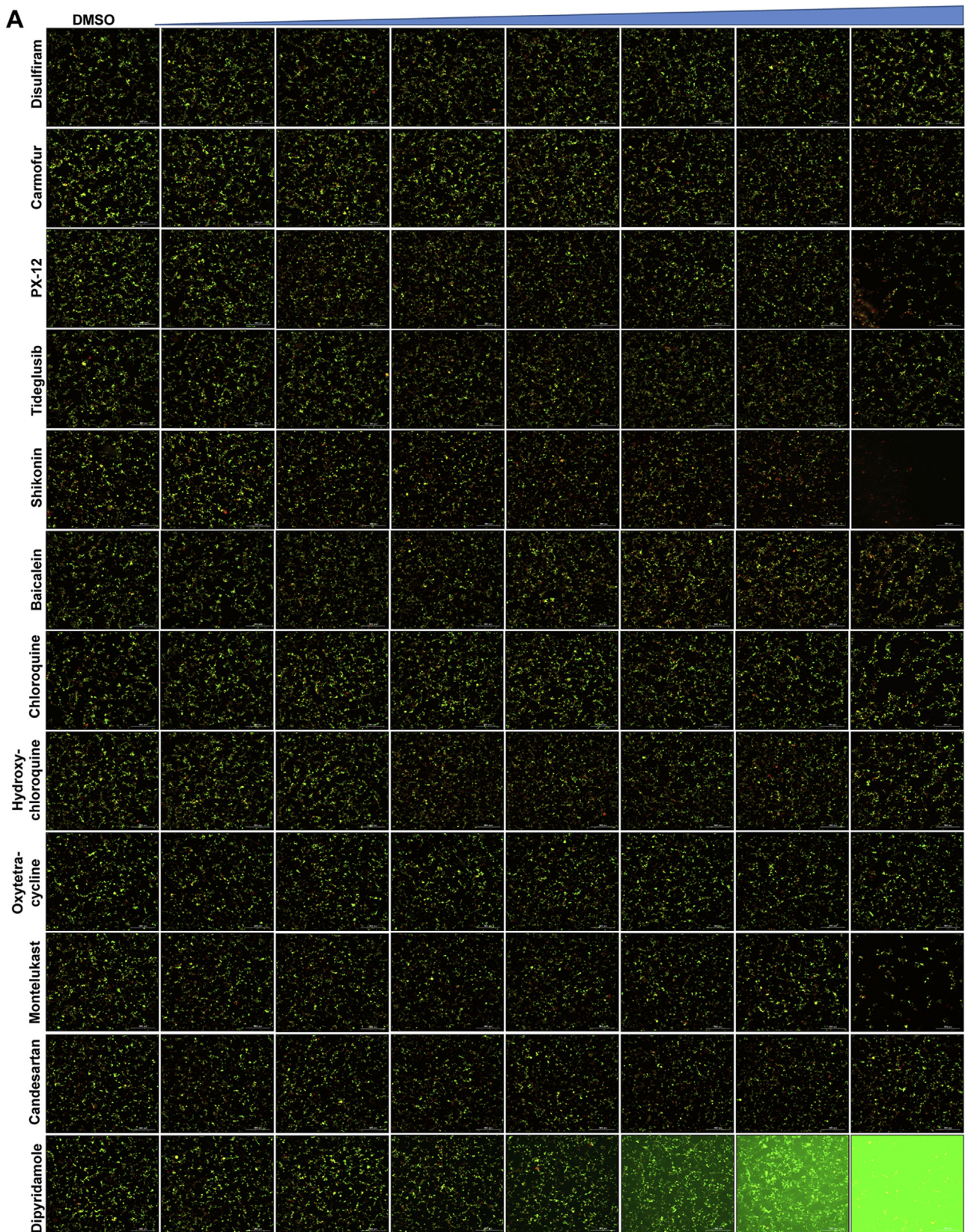


Figure 5 Validation/invalidation of disulfiram, carmofur, PX-12, tideglusib, shikonin, baicalein, chloroquine, hydroxychloroquine, oxytetracycline, montelukast, candesartan, and dipyridamole as SARS CoV-2 M^{Pro} inhibitors using the FlipGFP assay and Protease-Glo luciferase assay. (A) Representative images from the FlipGFP- M^{Pro} assay. The fluorescent background for dipyridamole at high drug concentrations (last row) was caused by the fluorescence emission from the compound itself. The scale bar is 300 μ m. (B)–(M) Dose–response curve of the ratio of GFP/

In the same screening which we identified boceprevir as a SARS-CoV-2 M^{Pro} inhibitor, calpain inhibitors II and XII were also found to have potent inhibition against M^{Pro} with IC₅₀ values of 0.97 and 0.45 μmol/L in the FRET assay². Both compounds showed binding to M^{Pro} in the thermal shift and native mass spectrometry binding assays. The Protease-Glo luciferase assay similarly confirmed the potent inhibition of calpain inhibitors II and XII against M^{Pro} with IC₅₀ values of 0.60 and 0.79 μmol/L, respectively (Fig. 4G and H). However, calpain inhibitor II had no effect on the cellular M^{Pro} activity as shown by the lack of inhibition in the FlipGFP assay (IC₅₀ > 60 μmol/L, Fig. 4A and C), while calpain inhibitor XII showed weak activity (IC₅₀ = 38.71 μmol/L, Fig. 4A and D). A recent study by Cao et al.⁴⁵ using a M^{Pro} triggered cytotoxicity assay similarly found the lack of cellular M^{Pro} inhibition by calpain inhibitors II and XII. These results contradict to the potent antiviral activity of both compounds in Vero E6 cells². It is noted that calpain inhibitors II and XII are also potent inhibitors of cathepsin L with IC₅₀ values of 0.41 and 1.62 nmol/L, respectively³. One possible explanation is that the antiviral activity of calpain inhibitors II and XII against SARS-CoV-2 might be cell type dependent, and the observed inhibition in Vero E6 cells might be due to cathepsin L inhibition instead of M^{Pro} inhibition. Vero E6 cells are TMPRSS2 negative, and SARS-CoV-2 enters cell mainly through endocytosis and is susceptible to cathepsin L inhibitors⁵⁶. To further evaluate the antiviral activity of calpain inhibitors II and XII against SARS-CoV-2, we tested them in Calu-3 cells using the immunofluorescence assay (Fig. 4J, K, and L). Calu-3 is TMPRSS2 positive and it is a close mimetic of the human primary epithelial cell⁵⁷. As expected, calpain inhibitors II and XII displayed much weaker antiviral activity against SARS-CoV-2 in Calu-3 cells than in Vero E6 cells with EC₅₀ values of 30.34 and 14.78 μmol/L, respectively (Fig. 4K and L). These results suggest that the FlipGFP assay can be used to faithfully predict the antiviral activity of M^{Pro} inhibitors. The lower activity of calpain inhibitors II and XII in the FlipGFP assay and the Calu-3 antiviral assay might due to the competition with host proteases, resulting in the lack of cellular target engagement with M^{Pro}.

In conclusion, calpain inhibitors II and XII are validated as M^{Pro} inhibitors but their antiviral activity against SARS-CoV-2 is cell type dependent. Accordingly, TMPRSS2 positive cell lines such as Calu-3 should be used to test the antiviral activity of calpain inhibitors II and XII analogs.

Ebselen is among one of the most frequently reported promiscuous M^{Pro} inhibitors. It was first reported by Jin et al.¹⁶ that ebselen inhibits SARS-CoV-2 M^{Pro} with an IC₅₀ of 0.67 μmol/L and the SARS-CoV-2 replication with an EC₅₀ of 4.67 μmol/L. However, it was noted that no reducing reagent was added in the FRET assay, and we reasoned that the observed inhibition might be due to non-specific modification of the catalytic cysteine 145 by ebselen. To test this hypothesis, we repeated the FRET assay

with and without reducing reagent DTT or GSH, and found that ebselen completely lost the M^{Pro} inhibition in the presence of DTT or GSH⁴¹. Similarly, ebselen also non-specifically inhibited several other viral cysteine proteases in the absence of DTT including SARS-CoV-2 PL^{Pro}, EV-D68 2A^{Pro} and 3C^{Pro}, and EV-A71 2A^{Pro} and 3C^{Pro}⁴¹. The inhibition was abolished with the addition of DTT. Ebselen also had no antiviral activity against EV-A71 and EV-D68, suggesting that the FRET assay results obtained without reducing reagent cannot be used to predict the antiviral activity. In this study, we found that ebselen showed no inhibition in either the FlipGFP assay or the Protease-Glo luciferase assay (Fig. 4A, E, and I), providing further evidence for the promiscuous mechanism of action of ebselen. Another independent study by Gurard-Levin et al.²⁶ using mass spectrometry assay reached similar conclusion that the inhibition of M^{Pro} by ebselen is non-specific and inhibition was abolished with the addition of reducing reagent DTT or glutathione. In contrary to the potent antiviral activity reported by Jin et al.¹⁶, the study from Gurard-Levin et al.²⁶ found that ebselen was inactive against SARS-CoV-2 in Vero E6 cells (EC₅₀ > 100 μmol/L). Chen et al.⁵⁸ reported that ebselen and disulfiram had synergistic antiviral effect with remdesivir against SARS-CoV-2 in Vero E6 cells. It was also proposed that ebselen and disulfiram act as zinc ejectors and inhibited not only the PL^{Pro}⁵⁹, but also the nsp13 ATPase and nsp14 exoribonuclease activities⁵⁸, further casting doubt on the detailed mechanism of action of ebselen.

Despite the accumulating evidence to support the promiscuous mechanism of action of ebselen, several studies continue to explore ebselen and its analogs as SARS-CoV-2 M^{Pro} and PL^{Pro} inhibitors^{42,60,61}. A number of ebselen analogs were designed and found to have comparable enzymatic inhibition and antiviral activity as ebselen. MR6-31-2 had slightly weaker enzymatic inhibition against SARS-CoV-2 M^{Pro} compared to ebselen (IC₅₀ = 0.824 vs. 0.67 μmol/L); however, MR6-31-2 had more potent antiviral activity than ebselen (EC₅₀ = 1.78 vs. 4.67 μmol/L) against SARS-CoV-2 M^{Pro} in Vero E6 cells. X-ray crystallization of SARS-CoV-2 M^{Pro} with MR6-31-2 (PDB: 7BAL) and ebselen (PDB: 7BAK) revealed nearly identical complex structures. It was found that selenium coordinates directly to Cys145 and forms a S–Se bond⁴². Accordingly, a mechanism involving hydrolysis of the organoselenium compounds was proposed. Similar to their previous study, the M^{Pro} enzymatic reaction buffer (50 mmol/L Tris pH 7.3, 1 mmol/L EDTA) did not include the reducing reagent DTT. Therefore, the M^{Pro} inhibition by these ebselen analogs might be non-specific and the antiviral activity might arise from other mechanisms⁴².

Overall, it can be concluded that ebselen is not a specific M^{Pro} inhibitor, and its antiviral activity against SARS-CoV-2 might involve other drug targets such as nsp13 or nsp14.

Disulfiram is an FDA-approved drug for alcohol aversion therapy. Disulfiram has a polypharmacology and was reported to inhibit multiple enzymes including urease⁶², methyltransferase⁶³, and kinase⁶² through reacting with cysteine residues. Disulfiram was also reported as an allosteric inhibitor of MERS-CoV PL^{Pro}⁶⁴.

mCherry fluorescent signal for disulfiram (B), carmofur (C), PX-12 (D), tideglusib (E), shikonin (F), baicalein (G), chloroquine (H), hydroxychloroquine (I), oxytetracycline (J), montelukast (K), candesartan (L), and dipyrindamole (M); mCherry signal alone was used to normalize protein expression level or calculate compound cytotoxicity. (N)–(Y) Protease-Glo luciferase assay results of disulfiram (N), carmofur (O), PX-12 (P), tideglusib (Q), shikonin (R), baicalein (S), chloroquine (T), hydroxychloroquine (U), oxytetracycline (V), montelukast (W), candesartan (X), and dipyrindamole (Y). Left column shows *Firefly* and *Renilla* luminescence signals in the presences of increasing concentrations of disulfiram, carmofur, PX-12, tideglusib, shikonin, baicalein, chloroquine, hydroxychloroquine, oxytetracycline, montelukast, candesartan, and dipyrindamole; Right column shows dose–response curve plots of the ratio of FFluc/Rluc luminescence. *Renilla* luminescence signal alone was used to normalize protein expression level. The results are mean ± standard deviation from three repeats. Compound concentration, μmol/L.

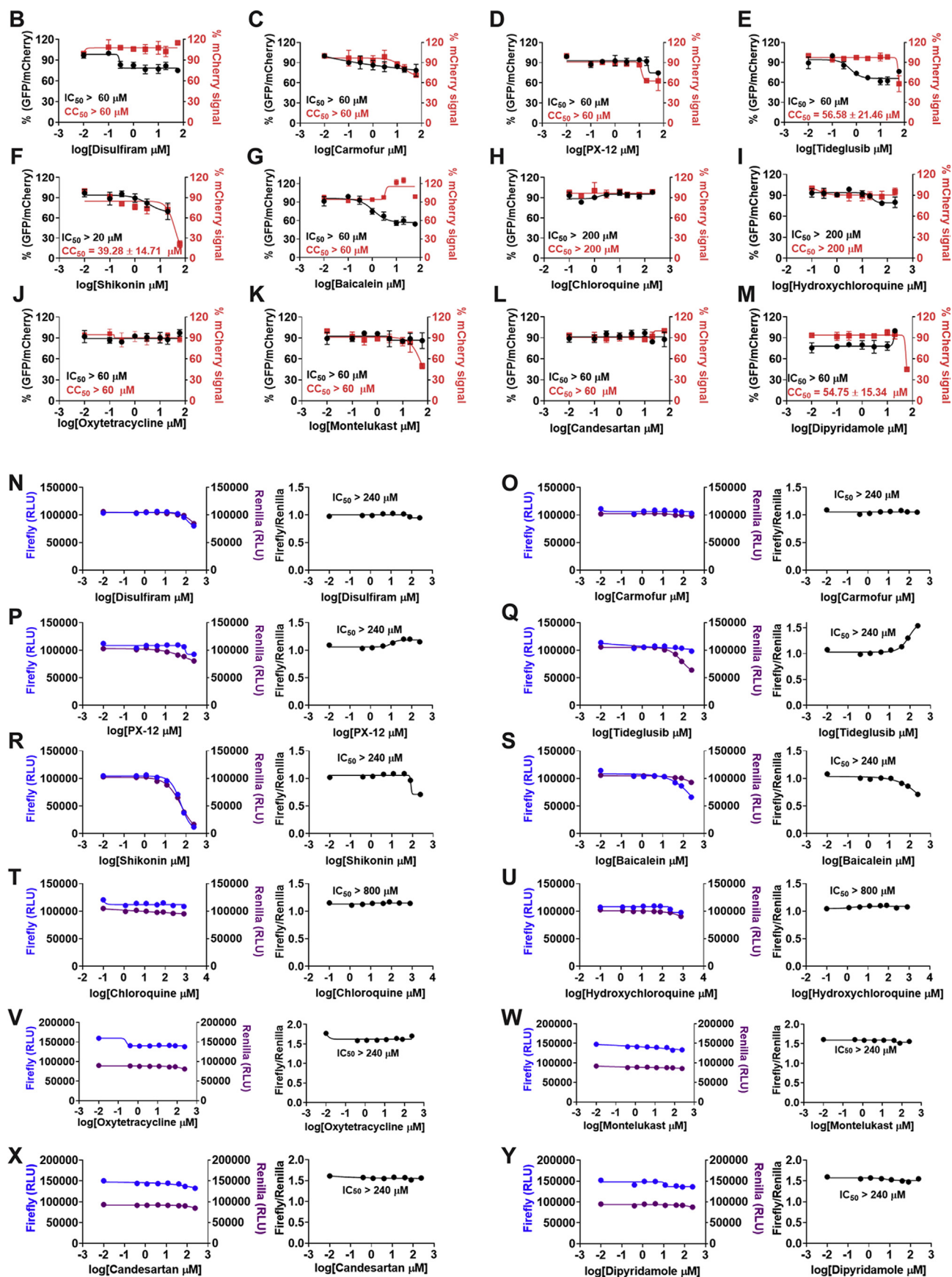


Figure 5 (continued)

Yang et al. reported disulfiram as a M^{pro} inhibitor with an IC₅₀ of 9.35 μmol/L. Follow up studies by us and others showed that disulfiram did not inhibit M^{pro} in the presence of DTT or GSH^{26,41}. In this study, disulfiram had no inhibition against M^{pro} in either the FlipGFP assay or the Protease-Glo luciferase assay (Fig. 5A, B and N).

Similar to disulfiram, carmofur, PX-12 and tideglusib, which were previously claimed by Jin et al.¹⁶ as M^{pro} inhibitors, showed no inhibitory activity in either the FlipGFP or Protease-Glo luciferase assay (Fig. 5A, C, D, E, O–Q), which is consistent with their lack of inhibition in the FRET assay in the presence of DTT.

Shikonin and baicalein are polyphenol natural products with known polypharmacology. Both compounds showed no inhibition in either the FlipGFP or the Protease-Glo luciferase assay (Fig. 5A, F, G, R, and S), suggesting they are not M^{pro} inhibitors. These two compounds were previously reported to inhibit SARS-CoV-2 M^{pro} in the FRET assay^{16,45,46} and had antiviral activity against SARS-CoV-2 in Vero E6 cells. However, our recent study showed that shikonin had no inhibition against SARS-CoV-2 M^{pro} in the FRET assay in the presence of DTT⁴¹. Studies from Gurard-Levin et al.²⁶ using FRET assay and mass spectrometry assay reached the same conclusion. X-ray crystal structure of SARS-CoV-2 M^{pro} in complex with shikonin showed that shikonin binds to the active site in a non-covalent manner⁴⁴.

In addition to the proposed mechanism of action of M^{pro} inhibition, Zandi et al.⁶⁵ showed that baicalein and baicalin inhibit the SARS-CoV-2 RNA-dependent RNA polymerase. Overall, shikonin and baicalein are not M^{pro} inhibitors and the antiviral activity of baicalein against SARS-CoV-2 might involve other mechanisms.

A recent study from Li et al.³⁷ identified several known drugs as SARS-CoV-2 M^{pro} inhibitors from a virtual screening. The identified compounds include chloroquine (IC₅₀ = 3.9 ± 0.2 μmol/L; K_i = 0.56 ± 0.12 μmol/L), hydroxychloroquine (IC₅₀ = 2.9 ± 0.3 μmol/L; K_i = 0.36 ± 0.21 μmol/L), oxytetracycline (IC₅₀ = 15.2 ± 0.9 μmol/L; K_i = 0.99 ± 0.06 μmol/L), montelukast (IC₅₀ = 7.3 ± 0.5 μmol/L), K_i = 0.48 ± 0.04 μmol/L), candesartan (IC₅₀ = 2.8 ± 0.3 μmol/L; K_i = 0.18 ± 0.02 μmol/L), and dipyridamole (K_i = 0.04 ± 0.001 μmol/L). The discovery of chloroquine and hydroxychloroquine as M^{pro} inhibitor was particularly intriguing. Several high-throughput screenings have been conducted for M^{pro}^{30,66}, and chloroquine and hydroxychloroquine were not among the list of active hits. In our follow up study, we found that none of the identified hits reported by Luo et al. inhibited M^{pro} either with or without DTT in the FRET assay⁵. In corroborate with our previous finding, the FlipGFP and Protease-Glo luciferase assays similarly confirmed the lack of inhibition of these compounds against M^{pro} (Fig. 5A, H–M, T–Y). Therefore, it can be concluded that chloroquine, hydroxychloroquine, oxytetracycline, montelukast, candesartan, and dipyridamole are not SARS-CoV-2 M^{pro} inhibitors. Other than the claims made by Luo et al., no other studies have independently confirmed these compounds as M^{pro} inhibitors.

4. Conclusions

The M^{pro} is perhaps the most extensive exploited drug target for SARS-CoV-2. A variety of drug discovery techniques have been applied to search for M^{pro} inhibitors. Researchers around the

world are racing to share their findings with the scientific community to expedite the drug discovery process. However, the quality of science should not be compromised by the speed. The mechanism of action of drug candidates should be thoroughly characterized in biochemical, binding, and cellular assays. Pharmacological characterization should address both target specificity and cellular target engagement. For target specificity, the drug candidates can be counter screened against unrelated cysteine proteases such as the viral EV-A71 2A^{pro}, EV-D68 2A^{pro}, the host cathepsins B, L, and K, caspases, calpains I, II, and III, etc. Compounds inhibit multiple cysteine proteases non-discriminately are most likely promiscuous compounds that act through redox cycling, inducing protein aggregation, or alkylating catalytic cysteine residue C145. For cellular target engagement, the FlipGFP and Protease-Glo luciferase assays can be applied. Both assays are performed in the presence of competing host proteins at the cellular environment. Collectively, our study reaches the following conclusions: 1) for validated M^{pro} inhibitors, the IC₅₀ values with and without reducing reagent should be about the same in the FRET assay; 2) validated M^{pro} inhibitors should show consistent results in the FRET assay, thermal shift binding assay, and the Protease-Glo luciferase assay. For compounds that are not cytotoxic, they should also be active in the FlipGFP assay; 3) compounds that have antiviral activity but lack consistent results from the FRET, thermal shift, FlipGFP, and Protease-Glo luciferase assays should not be classified as M^{pro} inhibitors; 4) compounds that non-specifically inhibit multiple unrelated viral or host cysteine proteases are most likely promiscuous inhibitors that should be triaged. 5) X-ray crystal structures cannot be used to justify the target specificity or cellular target engagement. Promiscuous compounds have been frequently co-crystallized with M^{pro} including ebselen, carmofur, and shikonin (Table 2). Overall, we hope our studies will promote the awareness of the promiscuous SARS-CoV-2 M^{pro} inhibitors among the scientific community and call for more stringent hit validation.

Acknowledgments

This research was supported by the National Institute of Allergy and Infectious Diseases at the National Institute of Health (NIH, USA; grants AII47325, AII57046, and AII58775) and the Arizona Biomedical Research Centre Young Investigator grant (ADHS18-198859, USA) to Jun Wang. The SARS-CoV-2 antiviral assay in Calu-3 cells was conducted by Drs. David Schultz and Sara Cherry at the University of Pennsylvania (USA) through the NIAID preclinical service under a non-clinical evaluation agreement.

Author contributions

Chunlong Ma performed the FlipGFP assay, Protease-Glo luciferase assay, and thermal shift assay with the assistance from Haozhou Tan. Juliana Choza and Yuyin Wang expressed the M^{pro} and performed the FRET assay. Jun Wang wrote the draft manuscript with the input from others; Jun Wang submitted this manuscript on behalf of other authors.

Conflicts of interest

The authors have no conflicts of interest to declare.

References

- Hu B, Guo H, Zhou P, Shi ZL. Characteristics of SARS-CoV-2 and COVID-19. *Nat Rev Microbiol* 2020;**19**:141–54.
- Ma C, Sacco MD, Hurst B, Townsend JA, Hu Y, Szeto T, et al. Boceprevir, GC-376, and calpain inhibitors II, XII inhibit SARS-CoV-2 viral replication by targeting the viral main protease. *Cell Res* 2020;**30**:678–92.
- Sacco MD, Ma C, Lagarias P, Gao A, Townsend JA, Meng X, et al. Structure and inhibition of the SARS-CoV-2 main protease reveal strategy for developing dual inhibitors against M^{pro} and cathepsin L. *Sci Adv* 2020;**6**:eabe0751.
- Gao X, Qin B, Chen P, Zhu K, Hou P, Wojdyla JA, et al. Crystal structure of SARS-CoV-2 papain-like protease. *Acta Pharm Sin B* 2021;**11**:237–45.
- Rut W, Groborz K, Zhang L, Sun X, Zmudzinski M, Pawlik B, et al. SARS-CoV-2 M^{pro} inhibitors and activity-based probes for patient-sample imaging. *Nat Chem Biol* 2021;**17**:222–8.
- Ghosh AK, Brindisi M, Shahabi D, Chapman ME, Mesecar AD. Drug development and medicinal chemistry efforts toward SARS-coronavirus and COVID-19 therapeutics. *ChemMedChem* 2020;**15**:907–32.
- Ullrich S, Nitsche C. The SARS-CoV-2 main protease as drug target. *Bioorg Med Chem Lett* 2020;**30**:127377.
- Vatansaver EC, Yang KS, Drelich AK, Kratch KC, Cho CC, Kempaiah KR, et al. Bepridil is potent against SARS-CoV-2 *in vitro*. *Proc Natl Acad Sci U S A* 2021;**118**:e2012201118.
- Gao S, Huang T, Song L, Xu S, Cheng Y, Cherukupalli S, et al. Medicinal chemistry strategies towards the development of effective SARS-CoV-2 inhibitors. *Acta Pharm Sin B* 2022;**12**:581–99.
- Xiang R, Yu Z, Wang Y, Wang L, Huo S, Li Y, et al. Recent advances in developing small-molecule inhibitors against SARS-CoV-2. *Acta Pharm Sin B* 2022;**12**:1591–622.
- Owen DR, Allerton CMN, Anderson AS, Aschenbrenner L, Avery M, Berritt S, et al. An oral SARS-CoV-2 M^{pro} inhibitor clinical candidate for the treatment of COVID-19. *Science* 2021;**374**:1586–93.
- Drayman N, DeMarco JK, Jones KA, Azizi SA, Froggatt HM, Tan K, et al. Masicitinib is a broad coronavirus 3CL inhibitor that blocks replication of SARS-CoV-2. *Science* 2021;**373**:931–6.
- Caceres CJ, Cardenas-Garcia S, Carnaccini S, Seibert B, Rajao DS, Wang J, et al. Efficacy of GC-376 against SARS-CoV-2 virus infection in the K18 hACE2 transgenic mouse model. *Sci Rep* 2021;**11**:9609.
- Dampalla CS, Zheng J, Perera KD, Wong LR, Meyerholz DK, Nguyen HN, et al. Postinfection treatment with a protease inhibitor increases survival of mice with a fatal SARS-CoV-2 infection. *Proc Natl Acad Sci U S A* 2021;**118**:e2101555118.
- Shi Y, Shuai L, Wen Z, Wang C, Yan Y, Jiao Z, et al. The preclinical inhibitor GS441524 in combination with GC376 efficaciously inhibited the proliferation of SARS-CoV-2 in the mouse respiratory tract. *Emerg Microb Infect* 2021;**10**:481–92.
- Jin Z, Du X, Xu Y, Deng Y, Liu M, Zhao Y, et al. Structure of M^{pro} from SARS-CoV-2 and discovery of its inhibitors. *Nature* 2020;**582**:289–93.
- Xia Z, Sacco M, Hu Y, Ma C, Meng X, Zhang F, et al. Rational design of hybrid SARS-CoV-2 main protease inhibitors guided by the superimposed cocrystal structures with the peptidomimetic inhibitors GC-376, telaprevir, and boceprevir. *ACS Pharmacol Transl Sci* 2021;**4**:1408–21.
- Ma C, Sacco MD, Xia Z, Lambrinidis G, Townsend JA, Hu Y, et al. Discovery of SARS-CoV-2 papain-like protease inhibitors through a combination of high-throughput screening and a FlipGFP-based reporter assay. *ACS Cent Sci* 2021;**7**:1245–60.
- Froggatt HM, Heaton BE, Heaton NS. Development of a fluorescence-based, high-throughput SARS-CoV-2 3CL^{pro} reporter assay. *J Virol* 2020;**94**:e01265-20.
- Li X, Lidsky P, Xiao Y, Wu C-T, Garcia-Knight M, Yang J, et al. Ethacridine inhibits SARS-CoV-2 by inactivating viral particles. *PLoS Pathog* 2021;**17**:e1009898.
- Kitamura N, Sacco MD, Ma C, Hu Y, Townsend JA, Meng X, et al. Expedited approach toward the rational design of noncovalent SARS-CoV-2 main protease inhibitors. *J Med Chem* 2022;**65**:2848–65.
- Zhang Q, Schepis A, Huang H, Yang J, Ma W, Torra J, et al. Designing a green fluorogenic protease reporter by flipping a beta strand of GFP for imaging apoptosis in animals. *J Am Chem Soc* 2019;**141**:4526–30.
- Wigdal SS, Anderson JL, Vidugiris GJ, Shultz J, Wood KV, Fan F. A novel bioluminescent protease assay using engineered firefly luciferase. *Curr Chem Genom* 2008;**2**:16–28.
- Xie X, Muruato AE, Zhang X, Lokugamage KG, Fontes-Garfias CR, Zou J, et al. A nanoluciferase SARS-CoV-2 for rapid neutralization testing and screening of anti-infective drugs for COVID-19. *Nat Commun* 2020;**11**:5214.
- Fu L, Ye F, Feng Y, Yu F, Wang Q, Wu Y, et al. Both boceprevir and GC376 efficaciously inhibit SARS-CoV-2 by targeting its main protease. *Nat Commun* 2020;**11**:4417.
- Gurard-Levin ZA, Liu C, Jekle A, Jaisinghani R, Ren S, Vandyck K, et al. Evaluation of SARS-CoV-2 3C-like protease inhibitors using self-assembled monolayer desorption ionization mass spectrometry. *Antivir Res* 2020;**182**:104924.
- Vuong W, Khan MB, Fischer C, Arutyunova E, Lamer T, Shields J, et al. Feline coronavirus drug inhibits the main protease of SARS-CoV-2 and blocks virus replication. *Nat Commun* 2020;**11**:4282.
- Bafna K, White K, Harish B, Rosales R, Ramelot TA, Acton TB, et al. Hepatitis C virus drugs that inhibit SARS-CoV-2 papain-like protease synergize with remdesivir to suppress viral replication in cell culture. *Cell Rep* 2021;**35**:109133.
- Kneller DW, Galanie S, Phillips G, O'Neill HM, Coates L, Kovalevsky A. Malleability of the SARS-CoV-2 3CL M^{pro} active-site cavity facilitates binding of clinical antivirals. *Structure* 2020;**28**:1313–1320.e3.
- Jan JT, Cheng TR, Juang YP, Ma HH, Wu YT, Yang WB, et al. Identification of existing pharmaceuticals and herbal medicines as inhibitors of SARS-CoV-2 infection. *Proc Natl Acad Sci U S A* 2021;**118**:e2021579118.
- Qiao J, Li YS, Zeng R, Liu FL, Luo RH, Huang C, et al. SARS-CoV-2 M^{pro} inhibitors with antiviral activity in a transgenic mouse model. *Science* 2021;**371**:1374–8.
- Kneller DW, Phillips G, Weiss KL, Zhang Q, Coates L, Kovalevsky A. Direct observation of protonation state modulation in SARS-CoV-2 main protease upon inhibitor binding with neutron crystallography. *J Med Chem* 2021;**64**:4991–5000.
- Bai Y, Ye F, Feng Y, Liao H, Song H, Qi J, et al. Structural basis for the inhibition of the SARS-CoV-2 main protease by the anti-HCV drug nlaraprevir. *Signal Transduct Target Ther* 2021;**6**:51.
- Hattori SI, Higshi-Kuwata N, Raghavaiah J, Das D, Bulut H, Davis DA, et al. GRL-0920, an indole chloropyridinyl ester, completely blocks SARS-CoV-2 infection. *mBio* 2020;**11**:e01833-20.
- Choy K-T, Wong AY-L, Kaewpreedee P, Sia SF, Chen D, Hui KPY, et al. Remdesivir, lopinavir, emetine, and homoharringtonine inhibit SARS-CoV-2 replication *in vitro*. *Antivir Res* 2020;**178**:104786.
- Ma C, Wang J. Dipyridamole, chloroquine, montelukast sodium, candesartan, oxytetracycline, and atazanavir are not SARS-CoV-2 main protease inhibitors. *Proc Natl Acad Sci U S A* 2021;**118**:e2024420118.
- Li Z, Li X, Huang YY, Wu Y, Liu R, Zhou L, et al. Identify potent SARS-CoV-2 main protease inhibitors *via* accelerated free energy perturbation-based virtual screening of existing drugs. *Proc Natl Acad Sci U S A* 2020;**117**:27381–7.
- Fintelman-Rodrigues N, Sacramento CQ, Ribeiro Lima C, Souza da Silva F, Ferreira AC, Mattos M, et al. Atazanavir, alone or in combination with ritonavir, inhibits SARS-CoV-2 replication and proinflammatory cytokine production. *Antimicrob Agents Chemother* 2020;**64**:e00825-20.
- Gupta A, Rani C, Pant P, Vijayan V, Vikram N, Kaur P, et al. Structure-based virtual screening and biochemical validation to discover a

- potential inhibitor of the SARS-CoV-2 main protease. *ACS Omega* 2020;**5**:33151–61.
40. Ghahremanpour MM, Tirado-Rives J, Deshmukh M, Ippolito JA, Zhang CH, Cabeza de Vaca I, et al. Identification of 14 known drugs as inhibitors of the main protease of SARS-CoV-2. *ACS Med Chem Lett* 2020;**11**:2526–33.
 41. Ma C, Hu Y, Townsend JA, Lagarias PI, Marty MT, Kolocouris A, et al. Ebselen, disulfiram, carmofur, PX-12, tideglusib, and shikonin are nonspecific promiscuous SARS-CoV-2 main protease inhibitors. *ACS Pharmacol Transl Sci* 2020;**3**:1265–77.
 42. Amporndanai K, Meng X, Shang W, Jin Z, Rogers M, Zhao Y, et al. Inhibition mechanism of SARS-CoV-2 main protease by ebselen and its derivatives. *Nat Commun* 2021;**12**:3061.
 43. Jin Z, Zhao Y, Sun Y, Zhang B, Wang H, Wu Y, et al. Structural basis for the inhibition of SARS-CoV-2 main protease by antineoplastic drug carmofur. *Nat Struct Mol Biol* 2020;**27**:529–32.
 44. Li J, Zhou X, Zhang Y, Zhong F, Lin C, McCormick PJ, et al. Crystal structure of SARS-CoV-2 main protease in complex with the natural product inhibitor shikonin illuminates a unique binding mode. *Sci Bull (Beijing)* 2021;**66**:661–3.
 45. Cao W, Cho CCD, Geng ZZ, Ma XR, Allen R, Shaabani N, et al. Cellular activities of SARS-CoV-2 main protease inhibitors reveal their unique characteristics. *bioRxiv* 2021. Available from: <https://doi.org/10.1101/2021.06.08.447613>.
 46. Su HX, Yao S, Zhao WF, Li MJ, Liu J, Shang WJ, et al. Anti-SARS-CoV-2 activities *in vitro* of Shuanghuanglian preparations and bioactive ingredients. *Acta Pharmacol Sin* 2020;**41**:1167–77.
 47. Wang M, Cao R, Zhang L, Yang X, Liu J, Xu M, et al. Remdesivir and chloroquine effectively inhibit the recently emerged novel coronavirus (2019-nCoV) *in vitro*. *Cell Res* 2020;**30**:269–71.
 48. Liu J, Cao R, Xu M, Wang X, Zhang H, Hu H, et al. Hydroxychloroquine, a less toxic derivative of chloroquine, is effective in inhibiting SARS-CoV-2 infection *in vitro*. *Cell Discov* 2020;**6**:16.
 49. Chu CM, Cheng VC, Hung IF, Wong MM, Chan KH, Chan KS, et al. Role of lopinavir/ritonavir in the treatment of SARS: initial virological and clinical findings. *Thorax* 2004;**59**:252–6.
 50. Cao B, Wang Y, Wen D, Liu W, Wang J, Fan G, et al. A trial of lopinavir–ritonavir in adults hospitalized with severe Covid-19. *N Engl J Med* 2020;**382**:1787–99.
 51. Group RC. Lopinavir–ritonavir in patients admitted to hospital with COVID-19 (RECOVERY): a randomised, controlled, open-label, platform trial. *Lancet* 2020;**396**:1345–52.
 52. Park SJ, Yu KM, Kim YI, Kim SM, Kim EH, Kim SG, et al. Antiviral efficacies of FDA-approved drugs against SARS-CoV-2 infection in Ferrets. *mBio* 2020;**11**:e01114–20.
 53. Zeldin RK, Petruschke RA. Pharmacological and therapeutic properties of ritonavir-boosted protease inhibitor therapy in HIV-infected patients. *J Antimicrob Chemother* 2004;**53**:4–9.
 54. Wu CY, Jan JT, Ma SH, Kuo CJ, Juan HF, Cheng YSE, et al. Small molecules targeting severe acute respiratory syndrome human coronavirus. *Proc Natl Acad Sci U S A* 2004;**101**:10012–7.
 55. O'Donnell HR, Tummino TA, Bardine C, Craik CS, Shoichet BK. Colloidal aggregators in biochemical SARS-CoV-2 repurposing screens. *bioRxiv* 2021. Available from: <https://doi.org/10.1101/2021.08.31.458413>.
 56. Hu Y, Ma C, Szeto T, Hurst B, Tarbet B, Wang J. Boceprevir, calpain inhibitors II and XII, and GC-376 have broad-spectrum antiviral activity against coronaviruses. *ACS Infect Dis* 2021;**7**:586–97.
 57. Hoffmann M, Kleine-Weber H, Schroeder S, Kruger N, Herrler T, Erichsen S, et al. SARS-CoV-2 cell entry depends on ACE2 and TMPRSS2 and is blocked by a clinically proven protease inhibitor. *Cell* 2020;**181**:271–280.e8.
 58. Chen T, Fei CY, Chen YP, Sargsyan K, Chang CP, Yuan HS, et al. Synergistic inhibition of SARS-CoV-2 replication using disulfiram/ebselen and remdesivir. *ACS Pharmacol Transl Sci* 2021;**4**:898–907.
 59. Sargsyan K, Lin CC, Chen T, Grauffel C, Chen YP, Yang WZ, et al. Multi-targeting of functional cysteines in multiple conserved SARS-CoV-2 domains by clinically safe Zn-ejectors. *Chem Sci* 2020;**11**:9904–9.
 60. Weglarz-Tomczak E, Tomczak JM, Talma M, Burda-Grabowska M, Giurg M, Brul S. Identification of ebselen and its analogues as potent covalent inhibitors of papain-like protease from SARS-CoV-2. *Sci Rep* 2021;**11**:3640.
 61. Sun LY, Chen C, Su J, Li JQ, Jiang Z, Gao H, et al. Ebsulfur and ebselen as highly potent scaffolds for the development of potential SARS-CoV-2 antivirals. *Bioorg Chem* 2021;**112**:104889.
 62. Galkin A, Kulakova L, Lim K, Chen CZ, Zheng W, Turko IV, et al. Structural basis for inactivation of *Giardia lamblia* carbamate kinase by disulfiram. *J Biol Chem* 2014;**289**:10502–9.
 63. Paranjpe A, Zhang R, Ali-Osman F, Bobustuc GC, Srivenugopal KS. Disulfiram is a direct and potent inhibitor of human O⁶-methylguanine–DNA methyltransferase (MGMT) in brain tumor cells and mouse brain and markedly increases the alkylating DNA damage. *Carcinogenesis* 2013;**35**:692–702.
 64. Lin MH, Moses DC, Hsieh CH, Cheng SC, Chen YH, Sun CY, et al. Disulfiram can inhibit MERS and SARS coronavirus papain-like proteases *via* different modes. *Antivir Res* 2018;**150**:155–63.
 65. Zandi K, Musall K, Oo A, Cao D, Liang B, Hassandarvish P, et al. Baicalein and baicalin inhibit SARS-CoV-2 RNA-dependent-RNA polymerase. *Microorganisms* 2021;**9**:893.
 66. Zhu W, Xu M, Chen CZ, Guo H, Shen M, Hu X, et al. Identification of SARS-CoV-2 3CL protease inhibitors by a quantitative high-throughput screening. *ACS Pharmacol Transl Sci* 2020;**3**:1008–16.